

Stability of circularly polarized Alfvén waves

Michael S. Ruderman

Department of Applied Mathematics, University of Sheffield
Hounsfield Road, Hicks Building
Sheffield S3 7RH, United Kingdom

Abstract. We consider one-dimensional motions of plasmas described by the system of ideal magnetohydrodynamic equations. We show that a circularly polarized one-dimensional Alfvén wave propagating along constant magnetic field is an exact solution of this system. The dispersion equations governing the stability of a circularly polarized Alfvén wave is derived. This equation is used to study the wave stability with respect to normal modes. The concept of absolute and convective instability is introduced. The recent results on the absolute and convective instability of circularly polarized Alfvén waves is presented and briefly discussed.

Keywords. Plasma, magnetohydrodynamics, waves, stability.

1. Introduction

Parametric instabilities of finite-amplitude circularly polarized Alfvén waves have been studied for the last four decades. They are interesting both from a purely theoretical point of view and from the point of view of applications to laboratory and space plasmas. The first analysis of the stability of a finite-amplitude circularly polarized Alfvén wave (the “pump wave”) carried out by Galeev & Oraevskii (1963) and Sagdeev & Galeev (1969) showed that this wave decays into a backward propagating Alfvén wave and a forward propagating sound wave. The analysis was based on the ideal MHD description and assumed that the plasma β and the pump wave amplitude are small. Derby (1978) and Goldstein (1978) also used the ideal MHD description to study the stability of circularly polarized Alfvén waves however with arbitrary amplitudes and in finite β plasmas. The stability analysis was further extended in different directions. Mio et al. (1976), Mjølhus (1976), Ovenden et al. (1983), and Spangler & Sheerin (1982, 1983) used the Derivative Nonlinear Schrödinger equation (DNLS) to study the stability of small-amplitude circularly polarized Alfvén waves in a dispersive plasma. Sakai & Sonnerup (1983), Longtin & Sonnerup (1986) and Wong & Goldstein (1986) used the two fluid description to take dispersion into account. Viñas & Goldstein (1991) studied the stability of a circularly polarized Alfvén wave with respect to non-one-dimensional perturbations. Hollweg et al. (1993) investigated the stability of a circularly polarized Alfvén wave in a three-component plasma consisting of electrons, protons and He^{++} ions. Ling & Abraham-Shrauner (1979), Spangler (1989) and Inhester (1990) used the kinetic description to study the stability of circularly polarized Alfvén waves. An excellent comparison of theory and observations is given in a review paper by Spangler (1997).

Although the stability of circularly polarized Alfvén waves has been studied for more than four decades, plasma physicists still pay much attention to this problem. Among recent publications we can mention the numerical investigations by Del Zanna et al. (2001), Del Zanna & Velli (2002) and Turkman & Torkelsson (2003, 2004), and the analysis of Alfvén wave stability in multicomponent and dusty plasmas by Hertzberg et al. (2003, 2004a,b) and Cramer et al. (2003).

In the traditional fluid treatment, the density perturbation is assumed to vary as

$\exp[i(kz - \omega t)]$. With this Ansatz for the density perturbation, the linearized MHD equations dictate how other quantities must vary. Jayanti & Hollweg (1993a) noticed that the linearized system of ideal MHD equations is a system with periodic coefficients and used Floquet's theorem to derive the dispersion equation determining the stability of a circularly polarized Alfvén wave in a Hall plasma. They obtained the same dispersion equation as Wong & Goldstein (1986) and Longtin & Sonnerup (1986). In the non-dispersive approximation corresponding to wavelengths much larger than the ion-inertia length this dispersion equation coincides with one obtained by Goldstein (1978) and Derby (1978). The derivation of the dispersion equation given by Jayanti & Hollweg (1993a) is fairly complicated. They first derived an infinite series of dispersion equations and then showed that, in fact, all of them are the same. Ruderman & Simpson (2004a) presented a new, more transparent method of deriving the dispersion equation. This method is also based on Floquet's theorem and consists of making the variable substitution that reduces the system of differential equations with periodic coefficients to the system with constant coefficients. As a result, similar to Jayanti & Hollweg (1993a), they also derived the dispersion equation without any *ad hoc* assumptions about the variation of the density perturbation, but in a much simpler way.

The dispersion equation for parametric instabilities of circularly polarized Alfvén waves is a complicated algebraic equation relating the frequency and wave-number of the density perturbation. This equation was mainly studied numerically (e.g., Wong & Goldstein 1986). The only extensive analytical study was carried out by Jayanti & Hollweg (1993b) who used either the amplitude of the pump-wave or the plasma beta, or the difference between the plasma beta and unity as a small parameter. Ruderman & Simpson (2004a) presented a qualitative analytical analysis of the dispersion equation valid for arbitrary values of the pump-wave amplitude.

Until recently only the normal mode analysis was used to study Alfvén wave stability. However, the normal mode analysis is not sufficient to conclude whether a wave appears stable or unstable in a fixed reference frame. The reason is that the normal mode analysis deals with spatially periodic perturbations, while real perturbations are bounded in space. To determine whether the wave appears stable or unstable in a fixed reference frame we have to solve the initial value problem for spatially bounded perturbations and then evaluate the asymptotic behaviour of the solution when the time tends to infinity. Then two scenarios are possible. In the first scenario the initial perturbation grows exponentially with time at any fixed spatial position. This situation is referred to as “absolute” instability. In the second scenario the initial perturbation grows exponentially with time, but simultaneously it is convected out of any finite spatial domain so fast that eventually it decays exponentially at any fixed spatial position. This situation is referred to as a “convective” instability.

The concept of absolute and convective instabilities was first introduced and developed in plasma physics (Briggs 1964; Bers 1973). Later it was applied to hydrodynamic stability problems (e.g. Kulikovskii & Shikina 1977; Huerre & Monkewitz 1985; Brevdo 1988; Ruderman 2000; Ruderman et al. 2004). Recently Ruderman & Simpson (2004b, 2006), Simpson & Ruderman (2005) and Simpson et al. (2006) studied the absolute and convective instabilities of circularly polarized Alfvén waves.

In this paper, we give the derivation of the dispersion equation determining the stability of circularly polarized Alfvén waves closely following to Ruderman & Simpson (2004a). Then we proceed to studying the absolute and convective instabilities of these waves and present the results obtained by Ruderman & Simpson (2004b, 2006), Simpson & Ruderman (2005) and Simpson et al. (2006).

2. Circularly polarized Alfvén waves

In what follows we use the system of ideal MHD equations. It consists of mass conservation equation,

$$\frac{\partial \rho}{\partial t} + \nabla \cdot (\rho \mathbf{v}) = 0, \quad (2.1)$$

momentum equation,

$$\frac{\partial \mathbf{v}}{\partial t} + (\mathbf{v} \cdot \nabla) \mathbf{v} = -\frac{\nabla p}{\rho} + \frac{1}{\mu_0 \rho} (\nabla \times \mathbf{B}) \times \mathbf{B}, \quad (2.2)$$

induction equation,

$$\frac{\partial \mathbf{B}}{\partial t} = \nabla \times (\mathbf{v} \times \mathbf{B}), \quad (2.3)$$

and adiabatic equation,

$$p = p_0 \left(\frac{\rho}{\rho_0} \right)^\gamma. \quad (2.4)$$

Here $\mathbf{v} = (u, v, w)$ is the velocity, $\mathbf{B} = (B_x, B_y, B_z)$ the magnetic field, ρ the density, and p the pressure; γ is the ration of specific heats, and μ_0 the magnetic permeability of free space.

Let us introduce Cartesian coordinates x, y, z , and consider solutions of system (2.1)–(2.4) that are independent of y and z . Then system (2.1)–(2.4) reduces to

$$\frac{\partial \rho}{\partial t} + \frac{\partial(\rho u)}{\partial x} = 0, \quad (2.5)$$

$$\frac{\partial u}{\partial t} + u \frac{\partial u}{\partial x} = -\frac{1}{\rho} \frac{\partial}{\partial x} \left(p + \frac{|\mathbf{B}_\perp|^2}{2\mu_0} \right), \quad (2.6)$$

$$\frac{\partial \mathbf{v}_\perp}{\partial t} + u \frac{\partial \mathbf{v}_\perp}{\partial x} = \frac{B_x}{\mu_0 \rho} \frac{\partial \mathbf{B}_\perp}{\partial x}, \quad (2.7)$$

$$\frac{\partial \mathbf{B}_\perp}{\partial t} = B_x \frac{\partial \mathbf{v}_\perp}{\partial x} - \frac{\partial(u \mathbf{B}_\perp)}{\partial x}, \quad (2.8)$$

$$p = p_0 \left(\frac{\rho}{\rho_0} \right)^\gamma, \quad (2.9)$$

where $\mathbf{v}_\perp = (0, v, w)$, $\mathbf{B}_\perp = (0, B_y, B_z)$, and $B_x = \text{const}$.

Let us consider a special class of solutions of the system (2.5)–(2.9) satisfying

$$\rho = \rho_0, \quad p = p_0, \quad u = 0, \quad |\mathbf{B}_\perp| = A = \text{const}. \quad (2.10)$$

Then equations (2.5), (2.6) and (2.9) are satisfied automatically, while equations (2.7) and (2.8) are transformed to

$$\frac{\partial \mathbf{v}_\perp}{\partial t} = \frac{B_x}{\mu_0 \rho_0} \frac{\partial \mathbf{B}_\perp}{\partial x}, \quad \frac{\partial \mathbf{B}_\perp}{\partial t} = B_x \frac{\partial \mathbf{v}_\perp}{\partial x}. \quad (2.11)$$

Eliminating \mathbf{v}_\perp from (2.11) we obtain

$$\frac{\partial^2 \mathbf{B}_\perp}{\partial t^2} - V_A^2 \frac{\partial^2 \mathbf{B}_\perp}{\partial x^2} = 0, \quad V_A^2 = \frac{B_x^2}{\mu_0 \rho_0}, \quad (2.12)$$

where V_A is the Alfvén speed. It follows from (2.10) that $B_y^2 + B_z^2 = A^2$, which implies that B_y and B_z can be written in the form

$$B_y = A \cos \phi, \quad B_z = A \sin \phi, \quad \phi = \phi(t, x). \quad (2.13)$$

Substituting (2.13) in (2.12) we obtain

$$\begin{aligned} \sin \phi \frac{\partial^2 \phi}{\partial t^2} + \cos \phi \left(\frac{\partial \phi}{\partial t} \right)^2 &= V_A^2 \left[\sin \phi \frac{\partial^2 \phi}{\partial x^2} + \cos \phi \left(\frac{\partial \phi}{\partial x} \right)^2 \right], \\ \cos \phi \frac{\partial^2 \phi}{\partial t^2} - \sin \phi \left(\frac{\partial \phi}{\partial t} \right)^2 &= V_A^2 \left[\cos \phi \frac{\partial^2 \phi}{\partial x^2} - \sin \phi \left(\frac{\partial \phi}{\partial x} \right)^2 \right]. \end{aligned} \quad (2.14)$$

After simple algebra this system of equations can be rewritten as

$$\frac{\partial^2 \phi}{\partial t^2} = V_A^2 \frac{\partial^2 \phi}{\partial x^2}, \quad \left(\frac{\partial \phi}{\partial t} \right)^2 = V_A^2 \left(\frac{\partial \phi}{\partial x} \right)^2. \quad (2.15)$$

It follows from the second equation in (2.15) that

$$\frac{\partial \phi}{\partial t} \pm V_A \frac{\partial \phi}{\partial x} = 0. \quad (2.16)$$

The sing + (−) corresponds to waves propagating in the positive (negative) direction of the x -axis. We consider waves propagating in the positive direction and take + in (2.16). Then it follows from (2.16) that $\phi = \phi(x - V_A t)$.

In what follows we take $\phi = k_0(x - V_A t)$. Then, using (2.11) and (2.13), we finally obtain $\mathbf{B}_\perp = \mathbf{B}_{0\perp}$, $\mathbf{v}_\perp = \mathbf{v}_{0\perp}$, where

$$\begin{aligned} B_{0y} &= A \cos[k_0(x - V_A t)], & B_{0z} &= A \sin[k_0(x - V_A t)], \\ v_{0y} &= -\frac{AV_A}{B_x} \cos[k_0(x - V_A t)], & v_{0z} &= -\frac{AV_A}{B_x} \sin[k_0(x - V_A t)]. \end{aligned} \quad (2.17)$$

We see that $\mathbf{B}_{0\perp}$ and $\mathbf{v}_{0\perp}$ are antiparallel. At fixed x the both vectors with angular velocity $|k_0|V_A$ clockwise (anti-clockwise) when $k_0 > 0$ ($k_0 < 0$). Fig. 1 illustrates the time dependence of vectors \mathbf{v}_\perp and \mathbf{B}_\perp determined by (2.17).

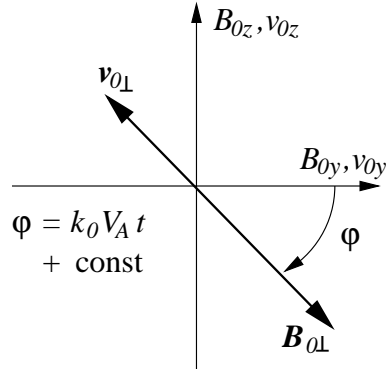


Figure 1. In a circularly polarized Alfvén wave $\mathbf{v}_{0\perp}$ is antiparallel to $\mathbf{B}_{0\perp}$. Both vectors rotate clockwise (anti-clockwise) when $k_0 > 0$ ($k_0 < 0$) with constant angular speed $|k_0|V_A$.

3. Derivation of dispersion equation

Let us write all dependent variables in the form $f = f_0 + f'$, where f_0 represents a circularly polarized Alfvén wave, and f' is perturbation. Substituting these expressions in (2.5)–(2.9) and linearizing the obtained equations, i.e. retain only terms linear with

respect to f' , we obtain

$$\frac{\partial \rho'}{\partial t} + \rho_0 \frac{\partial u'}{\partial x} = 0, \quad (3.1)$$

$$\frac{\partial u'}{\partial t} = -\frac{c_s^2}{\rho_0} \frac{\partial \rho'}{\partial x} - \frac{A}{\mu_0 \rho_0} \frac{\partial}{\partial x} (B'_y \cos \phi + B'_z \sin \phi), \quad (3.2)$$

$$\frac{\partial \mathbf{v}'_{\perp}}{\partial t} + u' \frac{\partial \mathbf{v}'_{0\perp}}{\partial x} = \frac{B_x}{\mu_0 \rho_0} \frac{\partial \mathbf{B}'_{\perp}}{\partial x} - \frac{B_x \rho'}{\mu_0 \rho_0^2} \frac{\partial \mathbf{B}_{0\perp}}{\partial x}, \quad (3.3)$$

$$\frac{\partial \mathbf{B}'_{\perp}}{\partial t} = B_x \frac{\partial \mathbf{v}'_{\perp}}{\partial x} - \frac{\partial (u' \mathbf{B}_{0\perp})}{\partial x}. \quad (3.4)$$

Here $c_s^2 = \gamma p_0 / \rho_0$ is the square of the sound speed. The system of equations (3.1)–(3.4) has variable coefficients. Let us introduce new variables

$$\begin{aligned} B_+ &= B'_y \cos \phi + B'_z \sin \phi, \\ B_- &= B'_y \sin \phi - B'_z \cos \phi \\ v_+ &= v'_y \cos \phi + v'_z \sin \phi, \\ v_- &= v'_y \sin \phi - v'_z \cos \phi. \end{aligned} \quad (3.5)$$

In new variables the system (3.1)–(3.4) takes the form

$$\frac{\partial \rho'}{\partial t} + \rho_0 \frac{\partial u'}{\partial x} = 0, \quad (3.6)$$

$$\frac{\partial u'}{\partial t} = -\frac{c_s^2}{\rho_0} \frac{\partial \rho'}{\partial x} - \frac{A}{\mu_0 \rho_0} \frac{\partial B_+}{\partial x}, \quad (3.7)$$

$$\frac{\partial v_+}{\partial t} - k_0 V_A v_- = \frac{B_x}{\mu_0 \rho_0} \left(\frac{\partial B_+}{\partial x} + k_0 B_- \right), \quad (3.8)$$

$$\frac{\partial v_-}{\partial t} + k_0 V_A v_+ + \frac{A V_A u'}{B_x} = \frac{B_x}{\mu_0 \rho_0} \left(\frac{\partial B_-}{\partial x} - k_0 B_+ + \frac{A k_0 \rho'}{\rho_0} \right), \quad (3.9)$$

$$\frac{\partial B_+}{\partial t} - k_0 V_A B_- = B_x \left(\frac{\partial v_+}{\partial x} + k_0 v_- \right) - A \frac{\partial u'}{\partial x}, \quad (3.10)$$

$$\frac{\partial B_-}{\partial t} + k_0 V_A B_+ = B_x \left(\frac{\partial v_-}{\partial x} - k_0 v_+ \right) + A k_0 u'. \quad (3.11)$$

This system has constant coefficients, so now we take all dependent variables proportional to $\exp[i(Kx - \Omega t)]$. As a result we obtain the system of algebraic equations

$$\Omega \rho' - \rho_0 K u' = 0, \quad (3.12)$$

$$\Omega u' - K \left(\frac{c_s^2}{\rho_0} \rho' + \frac{A}{\mu_0 \rho_0} B_+ \right) = 0, \quad (3.13)$$

$$\Omega v_+ - i k_0 V_A v_- + \frac{B_x}{\mu_0 \rho_0} (K B_+ - i k_0 B_-) = 0, \quad (3.14)$$

$$\Omega v_- + i k_0 V_A v_+ + \frac{i A V_A u'}{B_x} + \frac{B_x}{\mu_0 \rho_0} \left(K B_- + i k_0 B_+ - \frac{i A k_0 \rho'}{\rho_0} \right) = 0, \quad (3.15)$$

$$\Omega B_+ - i k_0 V_A B_- + B_x (K v_+ - i k_0 v_-) - A K u' = 0, \quad (3.16)$$

$$\Omega B_- + ik_0 V_A B_+ + B_x (K v_- + ik_0 v_+) + iA k_0 u' = 0. \quad (3.17)$$

(3.12)–(3.17) is a system of linear homogeneous algebraic equations. It has a non-trivial solution only when its determinant is zero. This condition given the dispersion equation

$$\begin{aligned} & \{(\Omega^2 - c_s^2 K^2)(\Omega - V_A K)[(\Omega + V_A K)^2 - 4V_A^2 k_0^2] - (A/B_x)^2 V_A^2 K^2 \\ & \times (\Omega^3 + V_A \Omega^2 K - 3V_A^2 \Omega k_0^2 + V_A^3 k_0^2 K)\}(\Omega - V_A K) = 0. \end{aligned} \quad (3.18)$$

The second multiplier in the dispersion equation (3.18) gives the solution $\Omega = V_A K$ which does not lead to instability. Hence we can disregard this multiplier. Then, introducing the dimensionless variables

$$a = \frac{A}{B_x}, \quad b = \frac{c_s}{V_A}, \quad k = \frac{K}{k_0}, \quad \omega = \frac{\Omega}{V_A k_0},$$

we rewrite the dispersion equation (3.18) as

$$D(k, \omega) \equiv (\omega^2 - b^2 k^2)(\omega - k) [(\omega + k)^2 - 4] - a^2 k^2 (\omega^3 + \omega^2 k - 3\omega + k) = 0 \quad (3.19)$$

4. Stability analysis

For any fixed k (3.19) is a fifth-order polynomial equation for ω . If all roots of this equation are real, then the perturbation with a fixed k is neutrally stable. Complex roots of (3.19) exist in complex conjugate pairs. This implies that, if not all roots are real, then the perturbation with the fixed k is unstable.

Let us introduce the dimensionless phase velocity $c = \omega/k$. Then (3.19) can be rewritten as

$$k^2 = F(c) \equiv \frac{G(c)}{(c+1)[c^4 - (1+a^2+b^2)c^2 + b^2]}, \quad (4.1)$$

where

$$G(c) = 4(c-1)(c^2 - b^2) - a^2(3c-1). \quad (4.2)$$

The dispersion equation (3.19) has five real roots if and only if the line $\xi = k^2$ in the $c\xi$ -plane has five intersections with the graph of the function $\xi = F(c)$. The graph of $F(c)$ for $a^2 = 1.4$ and $b = 0.5$ is displayed in Fig. 2. It can be shown that it remains qualitatively the same for any values of a and b satisfying $a^2 < 2(1 - b^2)$ (case *a*). The graph of $F(c)$ for $a^2 = 1.6$ and $b = 0.5$ is displayed in Fig. 3. It can be shown that it remains qualitatively the same for any values of a and b satisfying $a^2 > 2(1 - b^2)$ (case *b*).

We see that in both cases, *a*) and *b*), there are two quantities, ξ_1 and ξ_2 , such that there are five intersections of $\xi = k^2$ and $\xi = F(c)$ when either $\xi < \xi_1$ or $\xi > \xi_2$, and only three intersections when $\xi_1 < \xi < \xi_2$. Hence, we conclude that the circularly polarized Alfvén wave is unstable with respect to normal modes with the wave number k satisfying $\xi_1 < k^2 < \xi_2$. The dependencies of ξ_1 and ξ_2 on a are shown in Fig. 4. It can be shown that $\xi_1 \rightarrow 2^{-1/2} 3^{3/4} (3^{1/2} - 1) \approx 1.18$ and $\xi_2 \rightarrow \infty$ as $a \rightarrow \infty$.

When $b < 1$ ($c_s < V_A$) the instability of a circularly polarized Alfvén wave is called the *decay* instability. The reason is that, for $a \ll 1$, the instability is due to decay of a circularly polarized Alfvén wave (also called the pump wave) into a forward propagating sound wave and a backward propagating Alfvén wave. For $a \ll 1$ and b not very close to 0 and 1 the instability increment, γ_m , is given by (Jayanti & Hollweg 1993b)

$$\gamma_m = \frac{a\sqrt{1-b}}{2(1+b)\sqrt{b}} \quad (4.3)$$

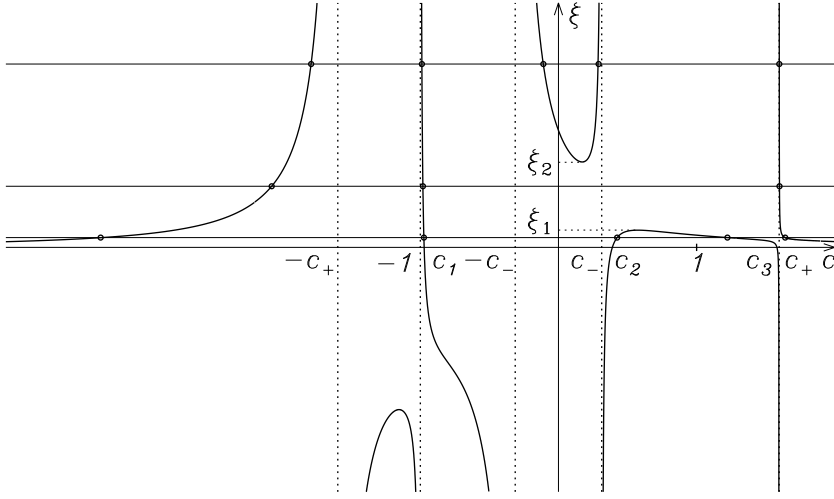


Figure 2. The graph of function $F(c)$ given by (4.1) for $a^2 = 1.4$ and $b = 0.5$. It is qualitatively the same for any values of a and b satisfying $a^2 < 2(1 - b^2)$. We see that there are five points of intersection and, consequently, five real roots of the dispersion equation when either $\xi < \xi_1$, or $\xi < \xi_2$. When $\xi_1 < \xi < \xi_2$, there are only three points of intersection and, consequently, only three real roots of the dispersion equation.

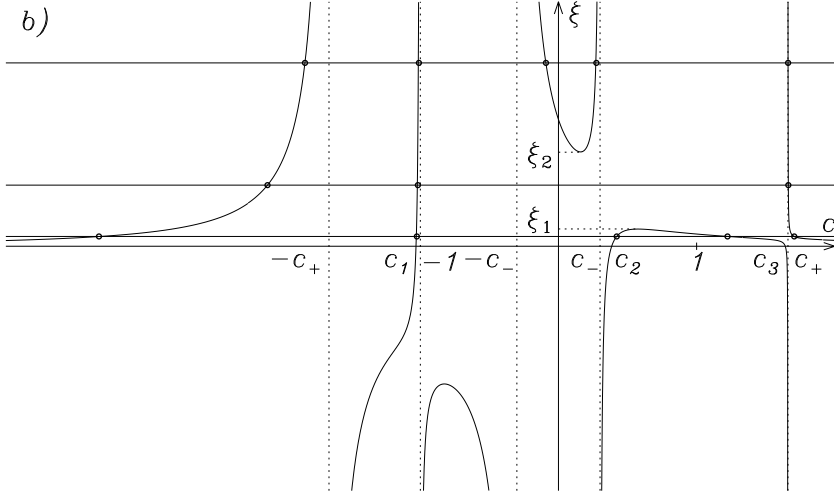


Figure 3. The graph of function $F(c)$ given by (4.1) for $a^2 = 1.6$ and $b = 0.5$. It is qualitatively the same for any values of a and b satisfying $a^2 > 2(1 - b^2)$. We see that there are five points of intersection and, consequently, five real roots of the dispersion equation when either $\xi < \xi_1$, or $\xi < \xi_2$. When $\xi_1 < \xi < \xi_2$, there are only three points of intersection and, consequently, only three real roots of the dispersion equation.

When $b > 1$ ($c_s > V_A$) the instability is called the beat instability because, for $a \ll 1$, the instability is due to beating of the pump wave with the sound wave which produces the forward and backward propagating Alfvén waves. For $a \ll 1$ and $b - 1 \sim 1$ the

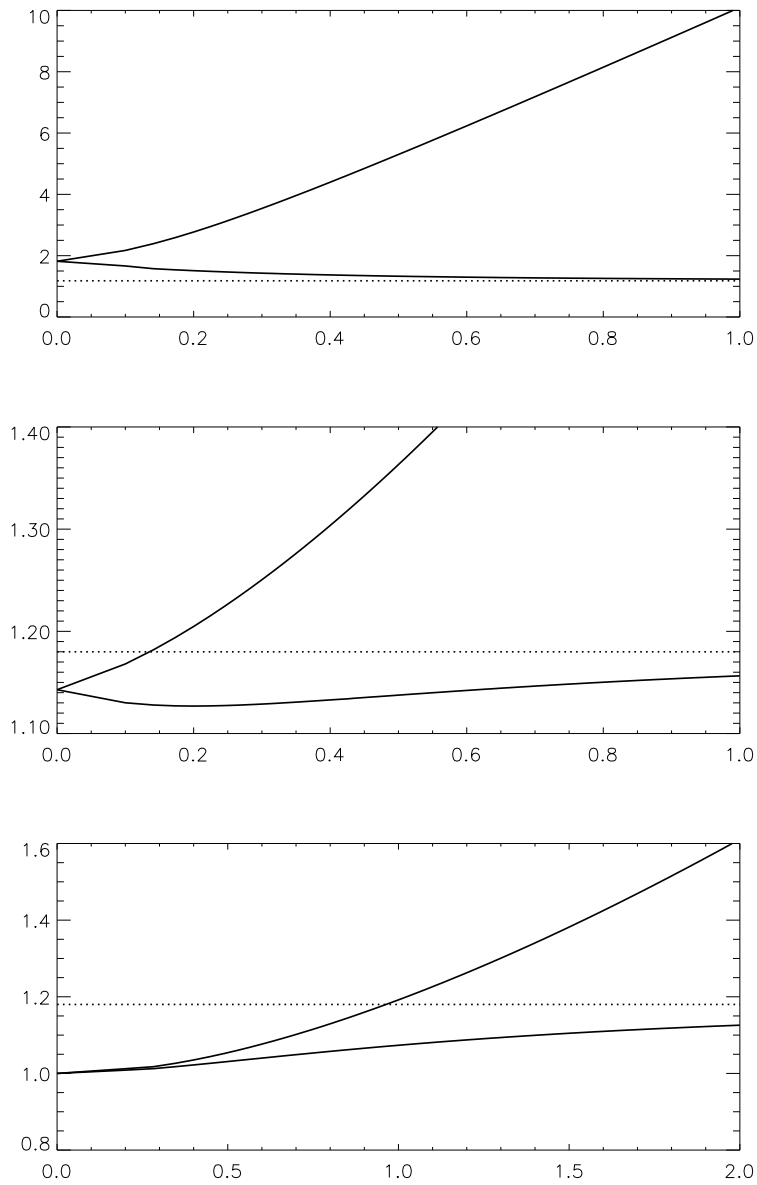


Figure 4. The dependencies of the boundaries of the instability interval with respect to the wavenumber, k_1 and k_2 , on a . The upper panel corresponds to $b = 0.1$, the middle panel to $b = 0.75$, and the lower panel to $b = 1.5$. The dependencies of k_1 and k_2 on a are qualitatively the same as in the upper panel when $b^2 < 1/3$, as in the middle panel when $1/3 < b^2 < 1$, and as in the lower panel when $b > 1$. The horizontal dotted lines are the asymptotes for $k_1(a)$ as $a \rightarrow \infty$.

instability increment is given by (Jayanti & Hollweg 1993b)

$$\gamma_m = \frac{a^3}{4\sqrt{2}(b^2 - 1)^{3/2}} \quad (4.4)$$

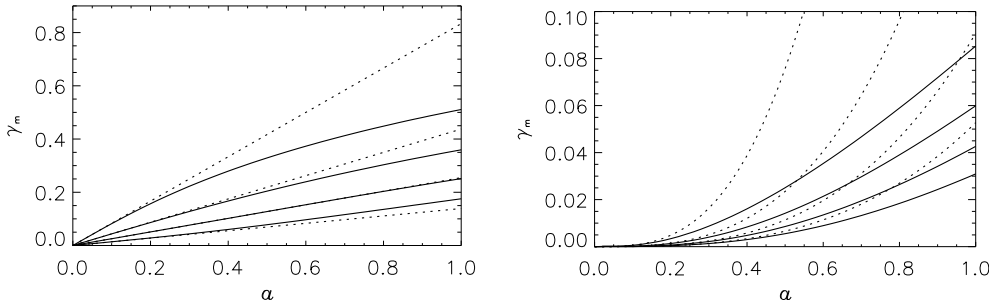


Figure 5. The increment γ_m versus a for the decay (left panel) and beat (right panel) instability. Solid (dashed) lines represent numerical (analytical) results for $b = 0.2$ (top line) in increments of 0.2 up to $b = 0.8$ (bottom line) in the left panel, and for $b = 1.2$ (top line) in increments of 0.2 up to $b = 1.8$ (bottom line) in the right panel.

We calculated γ_m for arbitrary a numerically. The results of these calculations are displayed in Fig. 5. The left panel corresponds to the decay instability, and the right to the beat instability. The solid curves show the numerically calculated dependencies of γ_m on a , and the dotted curves the dependencies given by equations (4.3) and (4.4).

5. Absolute and convective instabilities: general concept

The normal mode analysis is insufficient for describing the dynamics of localized perturbations. The only way to determine the dynamics of such perturbations is via an initial value problem. Two different cases of asymptotic behaviour of an initially localized perturbation of an unstable solution of MHD equations are possible. In the first case the perturbation grows exponentially in time at any fixed spatial location. This situation is referred to as an absolute instability. In the second case the perturbation as a whole also grows exponentially in time. However, it is convected out of any finite spatial domain so rapidly that eventually at every fixed spatial location an exponential decay is observed when $t \rightarrow \infty$. In the latter case the flow is said to be convectively unstable. The behaviour of a localized initial perturbation in the case of absolute and convectively instabilities is illustrated in Fig. 6. Note that the distinction between the absolute and convective instabilities is frame-dependent. The instability can be absolute in one reference frame, but convective in another.

Hence, to study absolute and convective instabilities we need to solve the initial value problem for linearized equations, in our case for equations (3.6)–(3.11). To do this we apply the Fourier transform with respect to x and the Laplace transform with respect to t to these equations written in a reference frame moving with the velocity \bar{U} with respect to the rest plasma. We find the solution of the transformed equations and then use the inverse Fourier and Laplace transform. As a result we obtain

$$\rho'(x, t) = \int_{i\tau-\infty}^{i\tau+\infty} e^{-i\omega t} d\omega \int_{-\infty}^{\infty} \frac{T(k, \omega)}{\tilde{D}(k, \omega)} e^{ikx} dk. \quad (5.1)$$

Here $\tilde{D}(k, \omega) = D(k, \tilde{\omega})$, where $D(k, \omega) = 0$ is the dispersion equation given by (3.19), $\tilde{\omega} = \omega + kU$ is the Doppler-shifted frequency and $U = \bar{U}/v_A$. $T(k, \omega)$ is determined by the initial conditions and is not important for what follows. $\Im(\omega) = \tau$ (\Im indicates the imaginary part of a quantity) is the Bromwich integration contour, $\tau > \gamma_m$. Perturbation of the other variables are given by similar expressions.

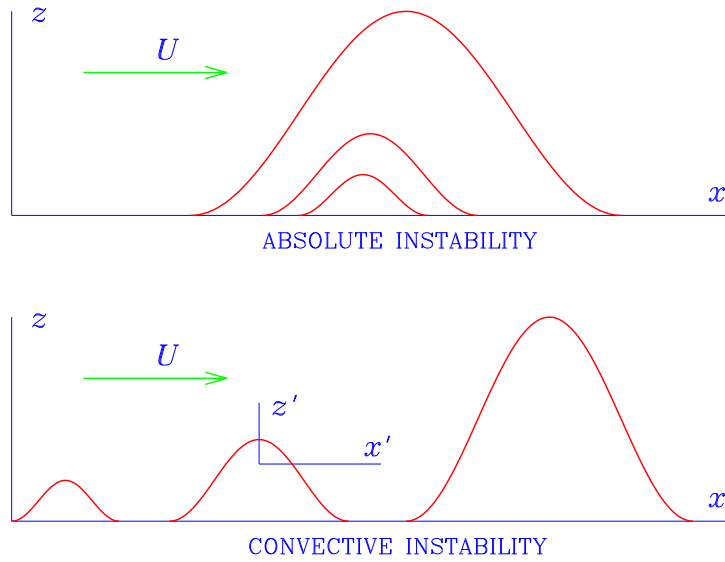


Figure 6. The behaviour of a localized perturbation in the case of absolute and convective instability. Note that, although the perturbation is convectively unstable in the reference frame xz , it is absolutely unstable in the reference frame $x'z'$.

To distinguish between the absolute and convective instabilities we need to study the asymptotic behaviour of $\rho'(x, t)$ as $t \rightarrow \infty$. To do this we are moving the Bromwich integration contour downward point by point. Let us write $\omega = \omega_r + i\omega_i$, fix ω_r and start to decrease ω_i . At the initial position there are no real roots of $\tilde{D}(k, \omega) = 0$ considered as an equation for k at fixed ω because $\tau > \gamma_m$. When the point ω in the complex ω -plane is moved down, the roots of equation $\tilde{D}(k, \omega) = 0$ move in the complex k -plane (see Fig. 7).

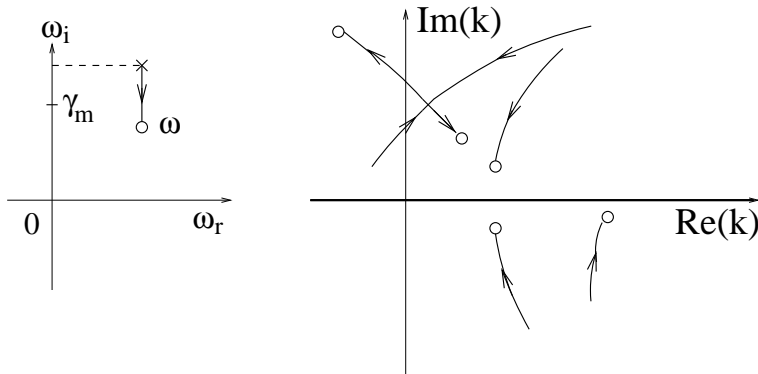


Figure 7. When the point ω in the complex ω -plane is moved down, the roots of equation $\tilde{D}(k, \omega) = 0$ move in the complex k -plane.

It can happen that one of the roots of equation $\tilde{D}(k, \omega) = 0$ crosses the real axis. In that case the integrand in (5.1) becomes singular and the integral with respect to k is divergent. To avoid this singularity we bend the integration contour in the complex k -plane (see Fig. 8). We can do this because the integrand in (5.1) is an analytic function of k .

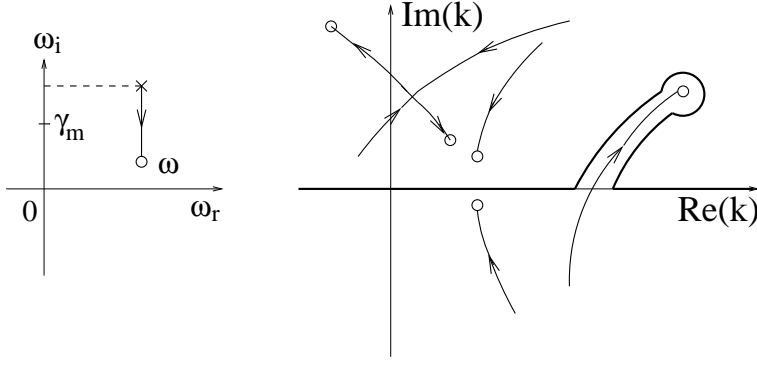


Figure 8. To avoid the singularity of the integrand in (5.1) we band the integration contour in the complex k -plane.

Eventually we can arrive at the situation when two roots coming from different sides of the integration contour “pinch” it (see Fig. 9). When colliding the two roots form a double root called pinching root.

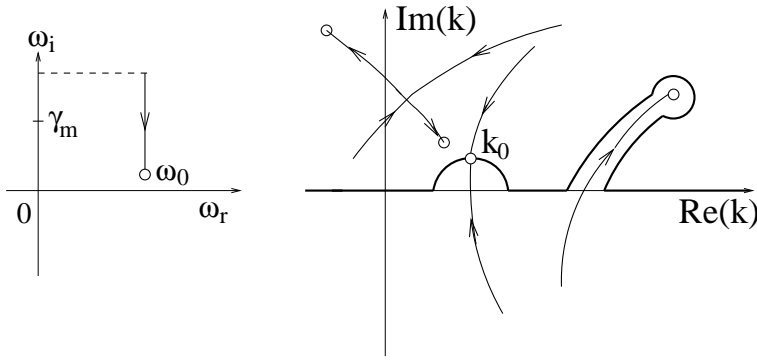


Figure 9. Two roots coming from different sides of the integration contour “pinch” it. When this happens, we cannot move ω down any longer.

The value of ω_i corresponding to pinching depends on ω_r . Let pinching occurs first time (i.e. for the largest value of ω_i) just when $\omega_r = \omega_{0r}$. Then all point of integration contour in the complex ω -plane can be moved below ω_0 , so that ω_0 is the apex point of the deformed contour.

To avoid singularity we have to stop moving the contour near ω_0 slightly before the pinching occurs. As a result we obtain the integration contour in the complex ω -plane shown in Fig. 10. The expression (4.1) transforms to

$$\rho'(x, t) = \int_{\mathcal{L}} e^{-i\omega t} d\omega \int_{\Gamma(\omega)} \frac{T(k, \omega)}{\tilde{D}(k, \omega)} e^{ikx} dk, \quad (5.2)$$

where $\Gamma(\omega)$ is the integration contour in the complex k -plane deformed to avoid singularities. Note that, in general, Γ depends on ω .

Let us introduce the notation

$$F(\omega, x) = \int_{\Gamma(\omega)} \frac{T(k, \omega)}{\tilde{D}(k, \omega)} e^{ikx} dk. \quad (5.3)$$

In a small vicinity of ω_0 we can take $\Gamma(\omega) = \Gamma(\omega_0)$. To calculate $F(\omega, x)$ we use the

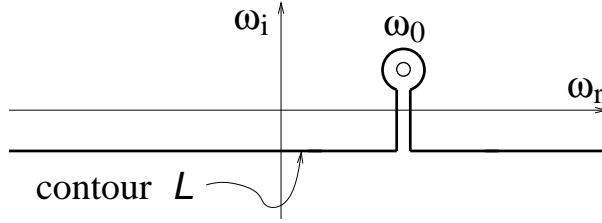


Figure 10. The sketch of the deformed integration contour in the complex ω -plane.

residue theorem. We consider the closed contour that consists of a part of $\Gamma(\omega_0)$ and the dashed line when $x > 0$, or the dotted line when $x < 0$. When the dashed line (dotted line) is moved to infinity, the integral along this line tends to zero. As a result the integral along $\Gamma(\omega_0)$ is equal to the sum of residues with respect to the poles inside the closed contour times $2\pi i \operatorname{sgn}(x)$, i.e.

$$\begin{aligned} F(\omega, x) &= 2\pi i \operatorname{sgn}(x) \sum_n \operatorname{res}_{k=k_n(\omega)} \left(\frac{T(k, \omega)}{\tilde{D}(k, \omega)} e^{ikx} \right) \\ &= 2\pi i \operatorname{sgn}(x) \sum_n \frac{T(k_n(\omega), \omega)}{\left. \frac{\partial \tilde{D}}{\partial k} \right|_{k=k_n(\omega)}} e^{ixk_n(\omega)}. \end{aligned} \quad (5.4)$$

In this expression the sum is taken over all zeros of $\tilde{D}(k, \omega)$ considered as a function of k in the upper (lower) part of complex k -plane when $x > 0$ ($x < 0$).

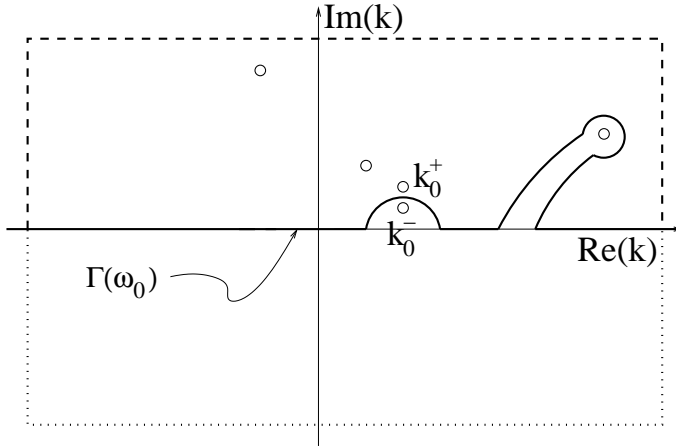


Figure 11. The closed contour consists of a part of $\Gamma(\omega_0)$ and the dashed line when $x > 0$, or the dotted line when $x < 0$.

Since k_0 is a double root of $\tilde{D}(k, \omega_0)$, $\frac{\partial \tilde{D}}{\partial k} = 0$ at $k = k_0$, $\omega = \omega_0$. Then the Taylor expansion of $\tilde{D}(k, \omega)$ near (k_0, ω_0) takes the form

$$\tilde{D}(k, \omega) = \left(\frac{\partial \tilde{D}}{\partial \omega} \right)_0 (\omega - \omega_0) + \frac{1}{2} \left(\frac{\partial^2 \tilde{D}}{\partial k^2} \right)_0 (k - k_0)^2 + \dots \quad (5.5)$$

Let us denote as $k_0^+(\omega)$ and $k_0^-(\omega)$ the two roots that collide and form the double root

k_0 , so that $k_0^\pm(\omega_0) = k_0$, $\Im(k_0^+(\omega)) > 0$, $\Im(k_0^-(\omega)) < 0$ when $\Im(\omega) > \gamma_m$. Then it follows from (5.5) that

$$k_0^\pm(\omega) \approx k_0 \pm \sqrt{g(\omega - \omega_0)}, \quad g = -2 \left(\frac{\partial \tilde{D}}{\partial \omega} \right)_0 / \left(\frac{\partial^2 \tilde{D}}{\partial k^2} \right)_0, \quad (5.6)$$

in a vicinity of ω_0 . Using (5.6) we obtain

$$\left. \frac{\partial \tilde{D}}{\partial k} \right|_{k=k_0^\pm} \approx \left(\frac{\partial^2 \tilde{D}}{\partial k^2} \right)_0 (k - k_0) = \pm \left(\frac{\partial^2 \tilde{D}}{\partial k^2} \right)_0 \sqrt{g(\omega - \omega_0)}. \quad (5.7)$$

We see that only the term with $k_n = k_0^+$ ($k_n = k_0^-$) is singular at $\omega = \omega_0$ in (5.4). Then it follows that in a small vicinity of ω_0 this term strongly dominates other terms, so that in this vicinity

$$F(\omega, x) \approx h(\omega - \omega_0)^{-1/2} e^{ik_0 x}, \quad h = \frac{2\pi i T(k_0, \omega_0)}{\left. \frac{\partial^2 \tilde{D}}{\partial k^2} \right|_0 \sqrt{g}}. \quad (5.8)$$

For large t the main contribution in the expression (5.2) for $\rho'(x, t)$ comes from the integral over the small circle with the centre at ω_0 . On this circle we can use the approximate expression (5.8). As a result, we obtain the asymptotic expression for $\rho'(x, t)$ valid for $t \rightarrow \infty$:

$$\rho'(x, t) = h e^{ik_0 x} \int_{\mathcal{C}} (\omega - \omega_0)^{-1/2} e^{-i\omega t} d\omega, \quad (5.9)$$

where \mathcal{C} is the circle of radius ε with the centre at ω_0 . We make the variable substitution $\omega = \omega_0 + \zeta/t$. Then

$$\int_{\mathcal{C}} (\omega - \omega_0)^{-1/2} e^{-i\omega t} d\omega = t^{-1/2} e^{-i\omega_0 t} \int_{\mathcal{C}_t} \zeta^{-1/2} e^{-i\zeta} d\zeta, \quad (5.10)$$

where \mathcal{C}_t is the circle of radius εt with the centre at the coordinate origin. Fig. 12 together with the residue theorem show that we can use the integration contour \mathcal{C}_1 instead of \mathcal{C}_t , where \mathcal{C}_1 has the radius ε .

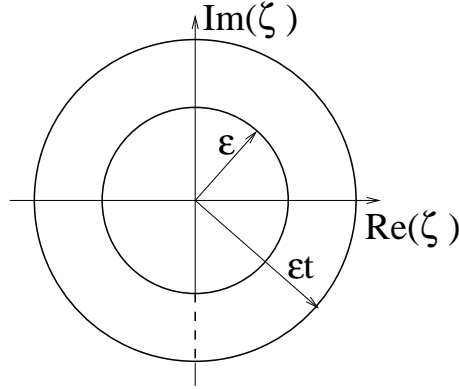


Figure 12. The integral along the closed contour that consists of the two circles and the connecting path shown by the dashed line is equal to zero. This implies that the integral along the circle of radius εt is equal to the integral along the circle of radius ε .

Equations (5.9) and (5.10) show that, as $t \rightarrow \infty$,

$$\rho'(x, t) = \text{const} \times t^{-1/2} \exp[i(k_0 x - \omega_0 t)]. \quad (5.11)$$

Hence, the instability is *absolute* if $\Im(\omega_0) > 0$, and *convective* if $\Im(\omega_0) \leq 0$. In accordance with our analysis we can divide studying the absolute and convective instabilities in the following five steps:

(i) Derive the dispersion equation using the normal mode analysis, and calculate the maximum growth rate of the instability γ_m .

(ii) Calculate all double-roots of the dispersion equation, which are determined by the system of two equations:

$$\tilde{D}(k, \omega) = 0, \quad \frac{\partial \tilde{D}}{\partial k} = 0. \quad (5.12)$$

The system of equations (5.12) determines double roots, k , and the corresponding values of ω .

(iii) Retain only those pairs of solutions to (5.12), (k, ω) , that satisfy the inequality

$$0 < \omega_i \leq \gamma_m. \quad (5.13)$$

If there are no such pairs, then the instability is *convective*.

(iv) Among all pairs (k, ω) satisfying (5.13) retain only those where k is a pinching double root. To verify that k is pinching, we fix $\Re(\omega)$ (\Re indicates the real part of a quantity) and increase $\Im(\omega)$ from ω_i to $\gamma_m + \epsilon$. We obtain the trajectories of the two k -roots that collide at the point k of the complex k -plane. If the end-points of these trajectories are on different sides of the real axis in the complex k -plane, then the double root is pinching. Otherwise it is non-pinching.

(v) Finally, among all pairs (k, ω) satisfying (5.13) and the condition that k is pinching, we choose one with the largest ω_i (of course it is possible that there are a few pairs with the same ω_i . In that case we can take any of them). Using the notation (k_0, ω_0) for this pair, we obtain that the asymptotic behaviour of the density perturbation is given by (5.11).

6. Absolute and convective instabilities: application to circularly polarized Alfvén waves

6.1. Decay instability ($c_s < V_A$)

Previously we used c to denote the phase velocity. Now we use it to denote Doppler-shifter phase velocity. So, in what follows, $c = \tilde{\omega}/k$. Now equation $\tilde{D}(k, \omega) = 0$ takes the form given by (4.1) and (4.2), and the system of two equations, (5.12), can be written as

$$k^2 = \frac{4(c-1)(c^2-b^2) - a^2(3c-1)}{(c+1)[c^4 - (1+a^2+b^2)c^2 + b^2]} \quad (6.1)$$

$$\begin{aligned} & 4(1+U)(c+1)(c-1)^2(c^2-b^2)^2 - a^2 \{ [c^6 + 4c^5 - 3c^4 - 2(1+3b^2)c^3 \\ & + 3b^2c^2 + 4b^2c - b^2] + U [6c^5 - 2c^4 - (5+7b^2)c^3 + 4b^2c^2 \\ & + (1+5b^2)c - 2b^2] \} + a^4 [2c^3 + U(3c^3 - c)] = 0 \end{aligned} \quad (6.2)$$

Equation (6.2) is the 7th order algebraic equation, so that it has 7 roots. For each root of (6.2) we will find two values of k from (6.1). For each k we obtain corresponding value of ω using $\omega = (c-U)k$. Hence, we have 14 pairs (k, ω) , where k is the double root of the dispersion equation, and ω is the corresponding value of frequency.

To make analytical progress we assume $a \ll 1$. Then it is possible to calculate all 14 pairs of (k, ω) and show that, when $-1 < U < b$, only 2 of them are pinching and satisfy the condition (5.13) (see Ruderman & Simpson 2004b). These roots are given by

$$k_{\pm} = \pm \frac{2}{1+b} + \frac{ia(1-b)^{1/2}(1-b+2U)}{2(1+b)^2[b(U+1)(b-U)]^{1/2}} + \mathcal{O}(a^2). \quad (6.3)$$

The corresponding values of ω are given by

$$\omega_{\pm} = \pm \frac{2(b-U)}{1+b} + \frac{ia[(1-b)(U+1)(b-U)]^{1/2}}{b^{1/2}(1+b)^2} + \mathcal{O}(a^2). \quad (6.4)$$

When $U < -1$ or $U > b$, there are no pinching roots satisfying (5.13). This implies that the instability is *absolute* when

$$-1 < U < b, \quad (6.5)$$

and *convective* otherwise. The instability increment takes its maximum value, $\Im(\omega_{\pm}) = \gamma_m$, when $U = (b-1)/2$.

6.2. Beat instability ($c_s > V_A$)

The analysis of the beat instability parallels to that of the decay instability (see Simpson & Ruderman 2005). Once again we solve the same system (6.1)–(6.2) and obtain 14 pairs of (k, ω) . When $-1 < U < 1$, only 2 of them are pinching and satisfy the condition (5.13). These roots are given by

$$k_{\pm} = \pm \left\{ 1 + \frac{a^2}{4(b^2-1)} \right\} + \frac{ia^3U}{4(b^2-1)^{3/2}[2(1-U^2)]^{1/2}} + \mathcal{O}(a^4). \quad (6.6)$$

The corresponding values of ω are given by

$$\omega_{\pm} = \pm \left\{ 1 - U - \frac{a^2(1+U)}{4(b^2-1)} \right\} + \frac{ia^3}{8} \left[\frac{2(1-U^2)}{(b^2-1)^3} \right]^{1/2} + \mathcal{O}(a^4). \quad (6.7)$$

When $U < -1$ or $U > 1$, there are no pinching roots satisfying (5.13). This implies that the instability is *absolute* when

$$-1 < U < 1, \quad (6.8)$$

and *convective* otherwise. The instability increment takes its maximum value, $\Im(\omega_{\pm}) = \gamma_m$, when $U = 0$.

6.3. Numerical results

Simpson et al. (2006) studied the decay instability numerically for arbitrary values of a . They found that, when a increases, the left boundary for U corresponding to the absolute instability also increases, while the right boundary decreases. Hence, the interval of values of U corresponding to the absolute instability shrinks (see Fig. 13).

In Fig. 14 the growth rate of the absolute instability is shown as a function of the reference frame velocity U . Comparison with the analytical results shows that the difference between the numerical and analytical results is small for $a = 0.2$, however it is getting bigger when a increases.

7. Application to solar wind

The solar wind speed is ~ 500 km/s, $V_A \sim 50$ km/s, the speed of any space station in the solar reference frame is much smaller than 500 km/s. This implies the following

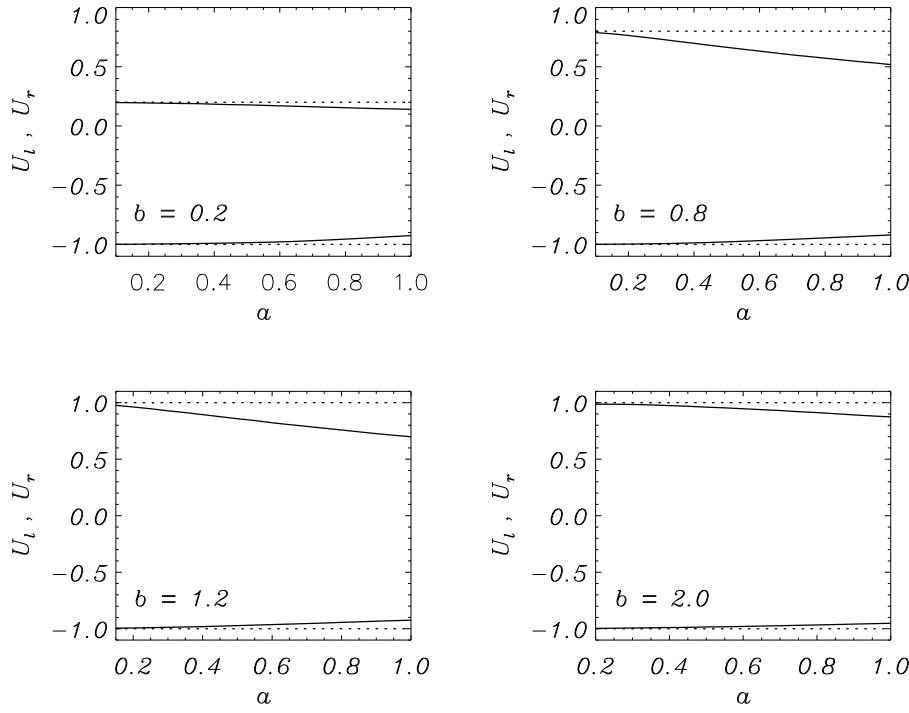


Figure 13. The solid lines show the numerically calculated dependencies of U_l (lower curves) and U_r (upper curves) on a for $b = 0.2, 0.8$, corresponding to the decay instability, and $b = 1.2, 2.0$, corresponding to the beat instability. The dotted lines show the analytical approximation for small a .

estimate for the speed $|\bar{U}|$ of the space station reference with respect to the rest plasma: $|\bar{U}| \sim 500$ km/s. Then for the dimensionless speed of the reference frame we obtain $|U| \sim 10$, so that $|U| \gg b, 1$. Therefore, in accordance with the results of the previous sections the instability observed by any space station is *convective* both when $b < 1$ and when $b > 1$.

Consider a circularly polarized Alfvén wave propagating in the anti-solar direction. Let its amplitude be $a = 0.2$, and its period in the solar wind reference frame 3 hours, which corresponds to $\omega_0 \approx 5.8 \times 10^{-4}$ s $^{-1}$. Assume that this wave is perturbed at a distance from the sun much smaller than 1 a.u. This perturbation will be convected from the sun by the solar wind. The time interval after which the perturbation arrives at the Earth orbit is $t_{\text{travel}} \approx 1$ a.u./ $(500$ km/s) $\approx 3 \times 10^5$ s. The dimensional increment of the perturbation is $\omega_0 \gamma_m$. Then its amplitude will increase by

$$\exp(\omega_0 \gamma_m t_{\text{travel}})$$

before it reaches the Earth orbit. Consider first the case when $c_s < V_A$ ($b < 1$), so that the instability is *decay*. In that case

$$\omega_0 \gamma_m t_{\text{travel}} \approx \frac{a\sqrt{1-b}}{2(1+b)\sqrt{b}} \omega_0 t_{\text{travel}} \approx 12$$

for $b \sim 0.5$, so that $\exp(\omega_0 \gamma_m t_{\text{travel}}) \approx 1.6 \times 10^5$, the perturbation amplitude is very large at the Earth orbit, so the perturbation attains the nonlinear regime.

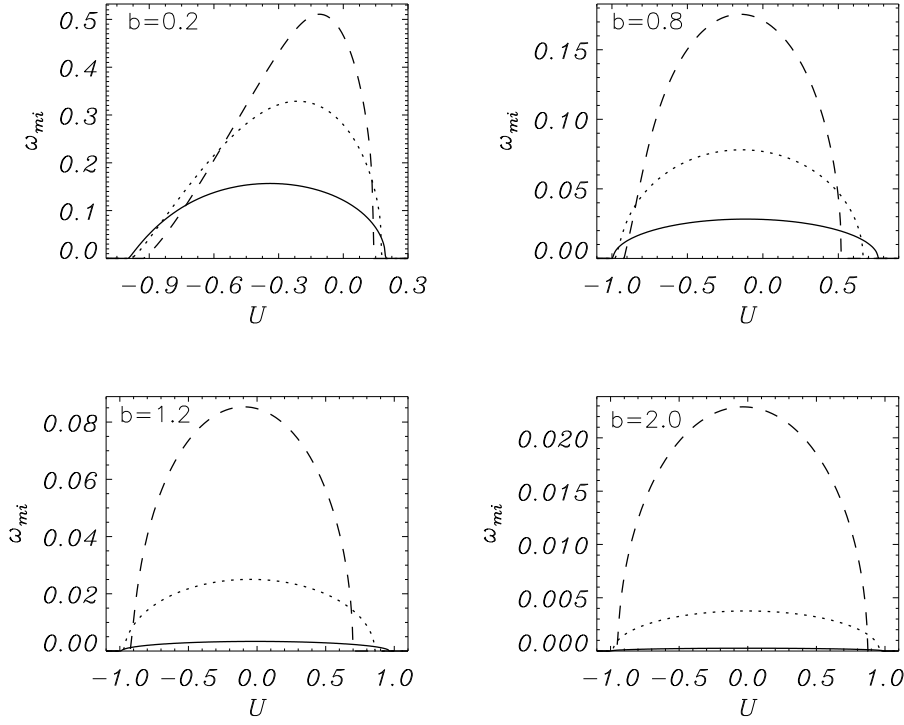


Figure 14. The growth rate of the absolute instability as a function of U for $a = 0.2$ (solid line), $a = 0.5$ (dotted line) and $a = 1$ (dashed line). Each panel represents a different value of b .

When $c_s > V_A$ ($b > 1$), so that the instability is *beat*, the similar estimates are

$$\omega_0 \gamma_m t_{\text{travel}} \approx \frac{a^3}{4\sqrt{2}(b^2 - 1)^{3/2}} \omega_0 t_{\text{travel}} \approx 0.05$$

for $b \sim 2$, so that $\exp(\omega_0 \gamma_m t_{\text{travel}}) \approx 1.05$. We see that the perturbation amplitude at the Earth orbit is almost the same as at the starting point, and the nonlinear effects will not be pronounced.

References

- Bers, A. 1973, in: *Survey Lectures. Proc. Int. Congr. Waves and Instabilities in Plasmas* (G. Auer & F. Cap, eds.), Institute for Theoretical Physics, Innsbruck, Austria, p. B1.
- Brevdo, L. 1988, *Geophys. Astrophys. Fluid Dynam.* **40**, 1.
- Briggs, R.J. 1964, *Electron-Stream Interaction with Plasmas* (Cambridge, MA: MIT Press).
- Cramer, N.F., Hertzberg, M.P. & Vladimirov, S.V. 2003, *Pramana-J. Phys.* **61**, 1171.
- Del Zanna, L., Velli, M. & Londrillo, P. 2001, *Astron. Astrophys.* **367**, 705.
- Del Zanna, L. & Velli, M. 2002, *Adv. Space. Res.* **30**, 471.
- Derby, N.F.J. 1978, *Astrophys. J.* **224**, 1013.
- Galeev, A.A. & Oraevskii, V.N. 1963, *Sov. Phys. Dokl.* **7**, 988.
- Goldstein, M.L. 1978, *Astrophys. J.* **219**, 700.
- Hertzberg, M.P., Cramer, N.F. & Vladimirov, S.V. 2003, *Phys. Plasmas* **10**, 3160.
- Hertzberg, M.P., Cramer, N.F. & Vladimirov, S.V. 2004a, *Phys. Rev. E* **69**, 056402.
- Hertzberg, M.P., Cramer, N.F. & Vladimirov, S.V. 2004b, *J. Geophys. Res.* **109**, A02103.
- Hollweg, J.V., Esser, R. & Jayanti, V. 1993, *J. Geophys. Res.* **98**, 3491.
- Huerre, P. & Monkewitz, P.A. 1985, *J. Fluid Mech.* **159**, 151.

- Inhester, B. 1990, *J. Geophys. Res.* **95**, 10525.
- Jayanti, V. & Hollweg, J.V. 1993a, *J. Geophys. Res.* **98**, 13247.
- Jayanti, V. & Hollweg, J.V. 1993b, *J. Geophys. Res.* **98**, 19049.
- Kulikovskii, A.G. & Shikina, I.C. 1977, *Izv. Akad. Nauk SSSR Mekh. Zhid. Gaza* **5**, 46.
- Ling, K.M. & Abraham-Shrauner, B. 1979, *J. Geophys. Res.* **84**, 6713.
- Longtin, M. & Sonnerup, B.U.Ö. 1986, *J. Geophys. Res.* **91**, 6816.
- Mio, J., Ogino, T., Minami, K. & Takeda, S. 1976, *J. Phys. Soc. Jpn.* **41**, 667.
- Mjølhus, E. 1976, *J. Plasma Phys.* **16**, 321.
- Ovenden, C.R., Shah, H.A. & Schwartz, S.J. 1983, *J. Geophys. Res.* **88**, 6095.
- Ruderman, M.S. 2000, *Astrophys. Space Sci.* **274**, 327.
- Ruderman, M.S. & Simpson, D. 2004a, *J. Plasma Phys.* **70**, 143.
- Ruderman, M.S. & Simpson, D. 2004b, *Phys. Plasmas* **11**, 4178.
- Ruderman, M.S. & Simpson, D. 2005, *Space Sci. Rev.* **121**, 287.
- Ruderman, M.S., Brevdo, L. & Erdélyi, R. 2004, *Proc. R. Soc. Lond. A* **460**, 847.
- Sagdeev, R.Z. & Galeev, A.A. 1969, *Non-Linear Plasma Theory* (New York: W.A. Benjamin).
- Sakai, J.I. & Sonnerup, B.U.Ö. 1983, *J. Geophys. Res.* **88**, 9069.
- Simpson, D. & Ruderman, M.S. 2005, *Phys. Plasmas* **12**, 062103.
- Simpson, D., Ruderman, M.S. & Erdélyi, R. 2006, *Astron. Astrophys.* **452**, 641.
- Spangler, S.R. 1989, *Phys. Fluids* **8**, 1738.
- Spangler, S.R. 1997, *Nonlinear Waves and Chaos in Space Plasmas* (T. Hada & H. Matsumoto, eds.), (Tokyo: TERRAPUB), p. 171.
- Spangler, S.R. & Sheerin, J.P. 1982, *J. Plasma Phys.* **27**, 193.
- Spangler, S.R. & Sheerin, J.P. 1983, *Astrophys. J.* **272**, 273.
- Turkman, R. & Torkelsson, U. 2003, *Astron. Astrophys.* **409**, 813.
- Turkman, R. & Torkelsson, U. 2004, *Astron. Astrophys.* **428**, 227.
- Viñas, A.F. & Goldstein, M.L. 1991, *J. Plasma Phys.* **46**, 129.
- Wong, H.K. & Goldstein, M.L. 1986, *J. Geophys. Res.* **91**, 5617.